Supporting Information

Noninvasive and Highly Multiplexed Five-Color Tumor Imaging of Multicore Near-Infrared Resonant Surface-Enhanced Raman Nanoparticles *in Vivo*

Jung Ho Yu[†,‡,*], *Idan Steinberg*[†,‡], *Ryan M. Davis*[†,‡], *Andrey V. Malkovskiy*[§], *Aimen Zlitni*[†,‡], *Rochelle Karina Radzyminski*[†,∥], *Kyung Oh Jung*[‡,⊥], *Daniel Tan Chung*[†,‡], *Luis Dan Curet*[†,‡], *Aloma L. D'Souza*[†,‡], *Edwin Chang*[†,‡], *Jarrett Rosenberg*[†], *Jos Campbell*[†,‡], *Hadas Frostig*[†,‡], *Seung-min Park*[†,‡], *Guillem Pratx*[‡,⊥], *Craig Levin*[†,‡], *and Sanjiv S. Gambhir*[†,‡,*]

[†]Department of Radiology, Stanford University School of Medicine, Stanford, California, 94305, United States. [‡]Molecular Imaging Program at Stanford (MIPS) and Bio-X Program, Stanford University, Stanford, California, 94305, United States. [§]Department of Plant Biology, Carnegie Institute for Science, Stanford, California, 94305, United States. [∥]Department of Applied Physics, Stanford University, Stanford, California, 94305, United States. [⊥]Department of Radiation Oncology, Stanford University School of Medicine, Stanford, California 94305, United States.

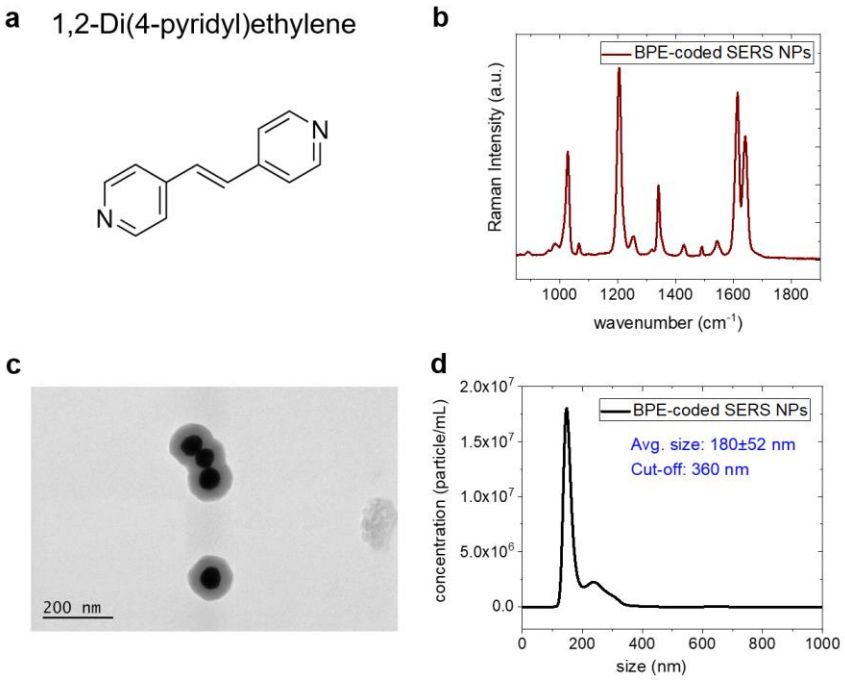

Figure S1. Characterization of non-resonant SERS nanoparticle of 1,2-Di(4-pyridyl)ethylene (BPE, S440, Oxonica Materials Inc.) (**a**) Molecular structure of the Raman reporter, BPE. (**b**) the Raman spectrum, (**c**) the TEM image, and (**d**) the nanoparticle tracking analysis result of BPE-coded SERS nanoparticles.

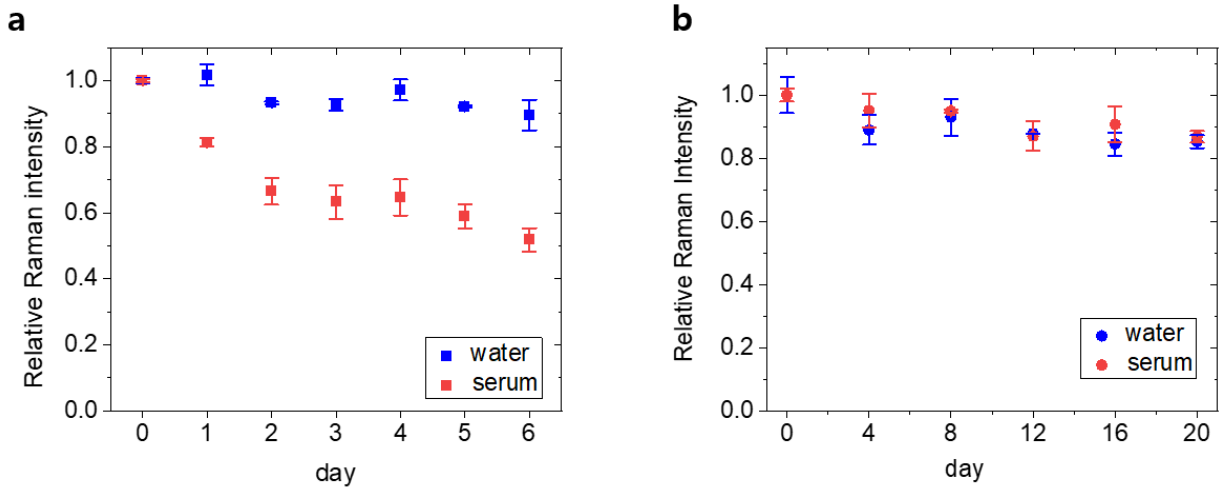

Figure S2. The stability of Raman signals from the DTTC-coded NIR-SERRS nanoparticles synthesized at room temperature (**a**) and at 60 ºC (**b**). Then the nanoparticles were placed in water (blue) and mouse serum (red) at 35 ºC. The error bars represent standard deviations of the Raman intensities collected from multiple samples (n=3).

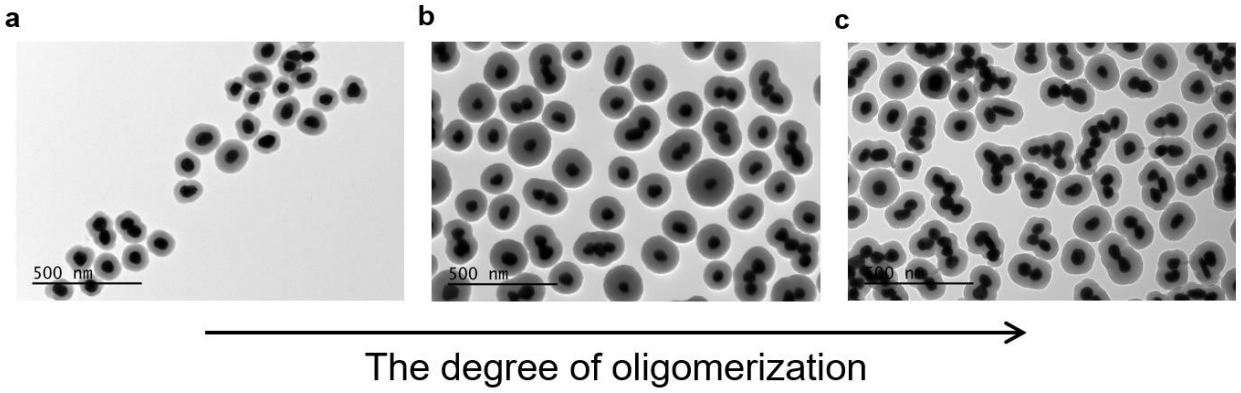

Figure S3. Controlled oligomerization of NIR-SERRS nanoparticles. Transmission electron microscope images of DTTC-coded NIR-SERRS nanoparticles oligomers, in which the degree of oligomerization increased from (**a**) to (**c**), upon the increase in the added DTTC dyes amount from 10 nmol (a), 15 nmol (b), to 20 nmol (c) during the syntheses. Scale bar: 500 nm.

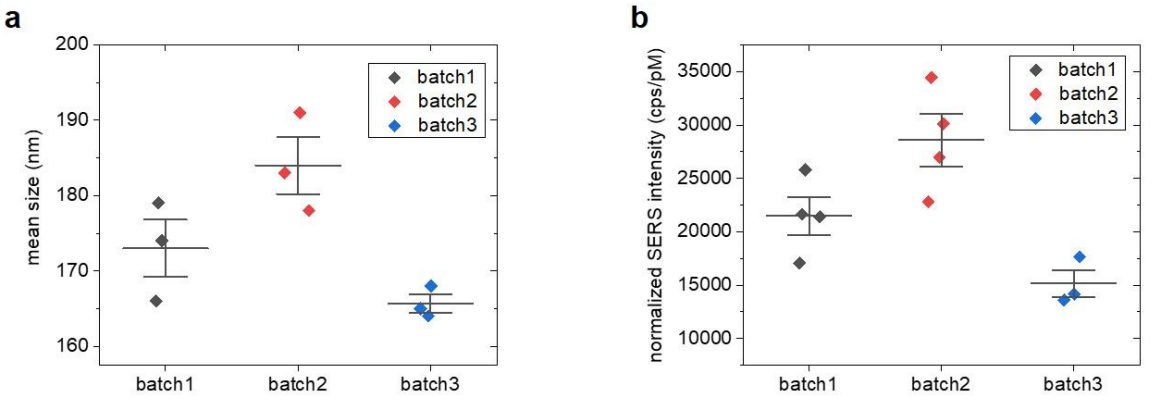

c

	ICC value between batches	ICC value within batches
SERS intensity	0.63	0.93
Mean size	0.61	0.93

Figure S4. Reproducibility of the NIR-SERRS nanoparticles synthesis. The measurement of the mean size (**a**) and the SERS intensity (**b**) of DTTC-coded NIR-SERRS nanoparticles reproduced by using the same or the different batches of gold nanoparticles. Each point represents the experimental data from the different batches of the NIR-SERRS nanoparticles production. (**c**) Intra-class correlation coefficients (ICCs) for the SERS intensity and the mean size of the reproduced nanoparticles when different batches (middle column) or the same batch (the right column) of gold nanoparticles are used. The ICC close to one indicates high similarity between values from the same group, while a low ICC close to zero means that values from the same group are not similar. From the ICC values, we conclude that the average size and the SERS intensity of the multicore NIR-SERRS nanoparticles were highly reproducible as long as the same batch of gold nanoparticle solution was used (ICC=0.93). On the other hand, there were variations of the average sizes (ICC=0.61) and the SERS signal intensities (IC=0.63) only when the different batches of gold nanoparticle solution were used for the synthesis.

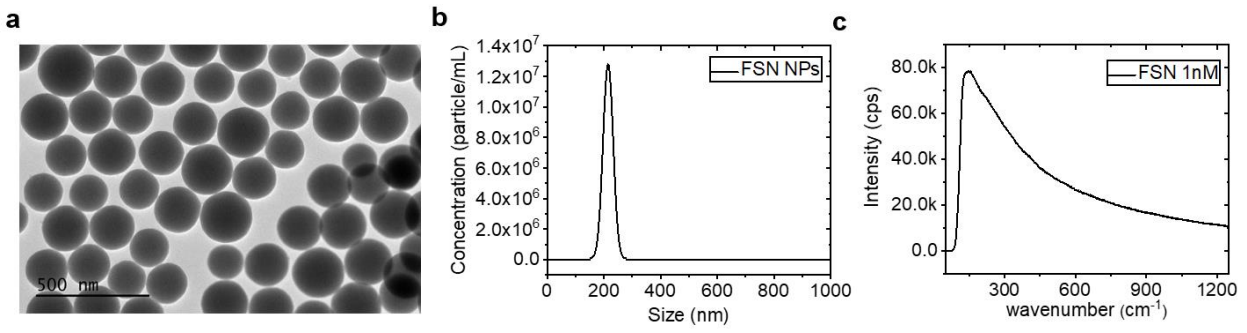

Figure S5. Characterization of Cy7-doped NIR-fluorescent silica nanoparticles. (**a**) A TEM image of the Cy7-doped silica nanoparticles (scale bar: 500 nm), (**b**) the nanoparticle tracking analysis result, and (**c**) NIR fluorescence spectrum of Cy7 dye-doped NIR-fluorescent silica nanoparticles (215±18 nm). The fluorescence spectrum was collected from the same Raman microscope used for the analysis of the NIR-SERRS nanoparticles.

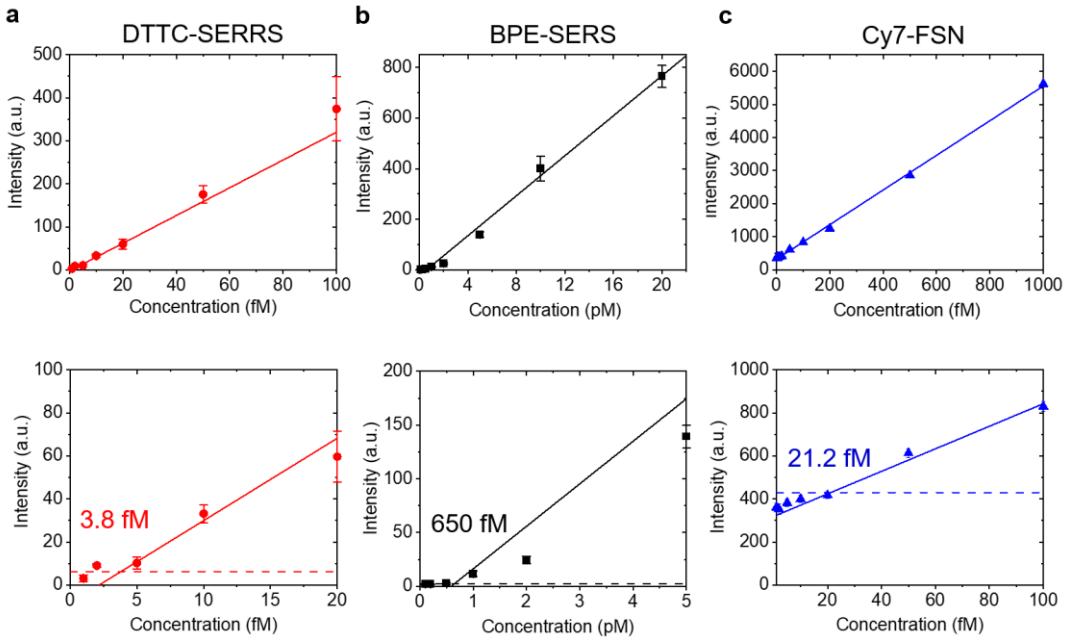

Figure S6. Limit of detections (LODs) calculated from the low concentration regime of the standard curves. (**a-c**) Linear plots of the emission intensities (upper panels) and the low concentration regime of the plots (lower panels) *vs*. concentration for the Raman scattering of DTTC-coded SERRS nanoparticles (a), the BPE-coded SERS nanoparticles (b), and for the fluorescence of the Cy7-doped fluorescent silica nanoparticles (c). The limits of detections (LODs) were calculated from the extrapolation of the linear plots to the points, which intersect four times the standard deviation of the background signals (horizontal line in each plot). The error bars represent standard deviations of the Raman intensities collected from multiple points (n=300) scanning per measurement.

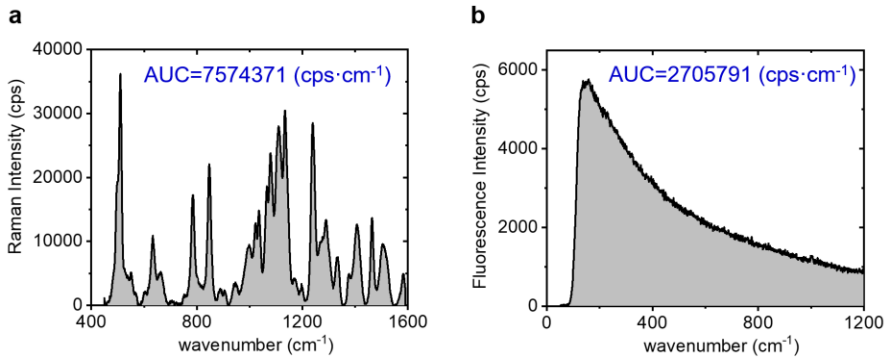

Figure S7. Comparison of brightness for the NIR-SERRS nanoparticles and the fluorescent silica nanoparticles. (**a**) A Raman spectrum of the DTTC-coded NIR-SERRS nanoparticles after fluorescent background subtraction. (**b**) A fluorescence spectrum of the Cy7-doped NIR-fluorescent silica nanoparticles. Both spectra were measured at the same concentration (1 pM) and instrumentation. Area under the curve (AUC) values were calculated from the integration of the spectra (grey areas).

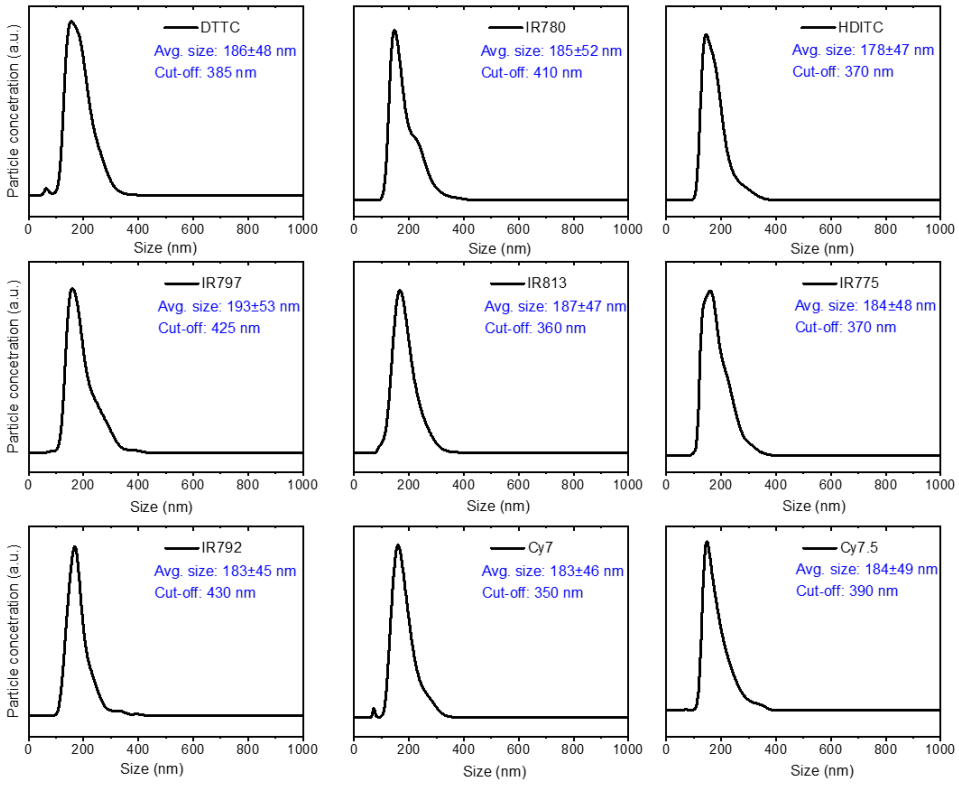

Figure S8. The size distribution of the 9 NIR-SERRS nanoparticles. The nanoparticle tracking analysis (NTA) results of the 9 multispectral NIR-SERRS nanoparticles, which were analyzed in Figure 2h (main text). We adjusted the average size and cut-off size of the NIR-SERRS nanoparticles to ~200 nm and ~400 nm, respectively, through the controlled oligomerization of gold nanoparticles.

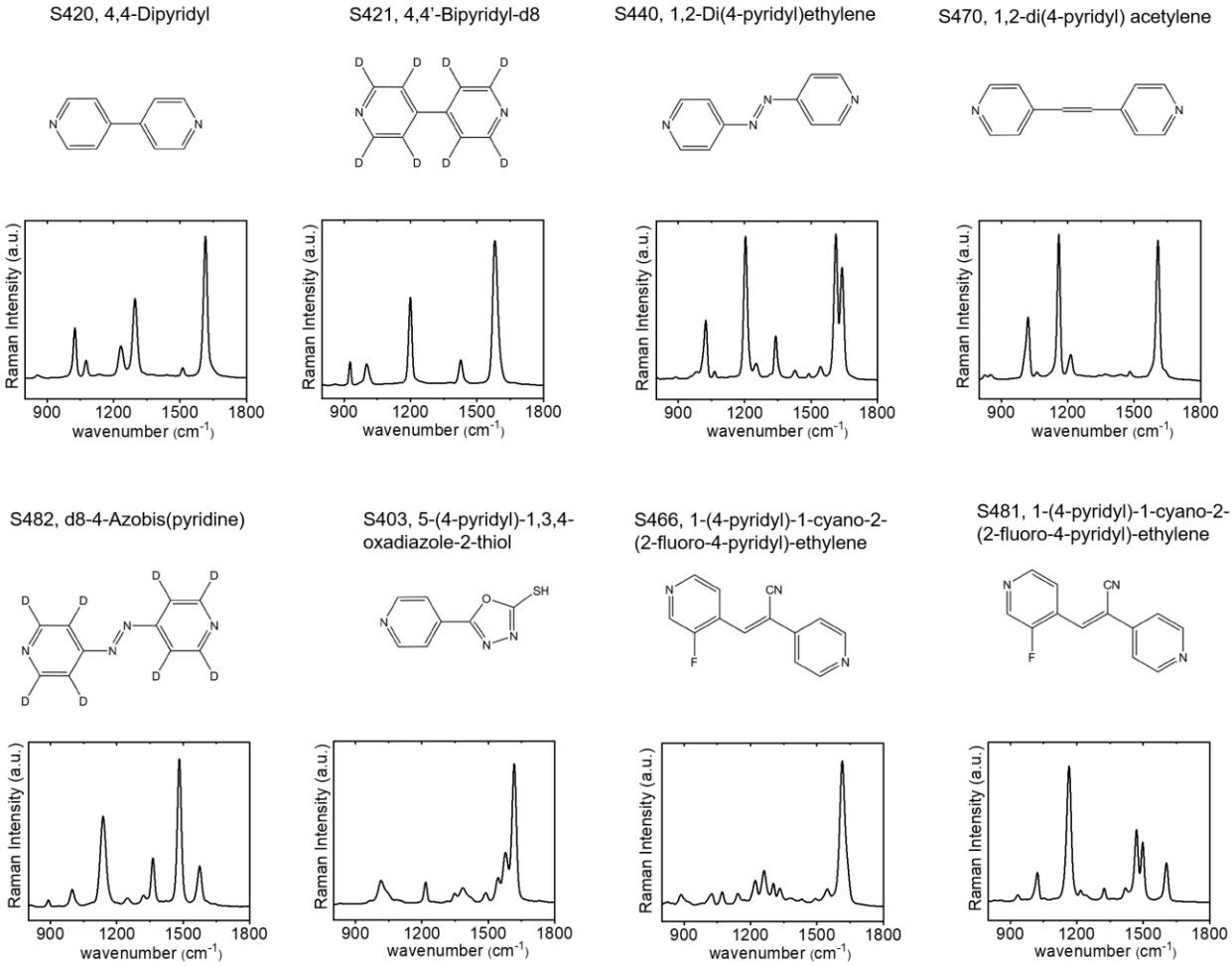

Figure S9. Non-resonant SERS spectra. Molecular structures of the non-resonant Raman reporters and the representative Raman spectra of the non-resonant SERS nanoparticles (Oxonica Materials Inc.). These Raman spectra were employed for the condition number analysis in Figure 3a (main text).

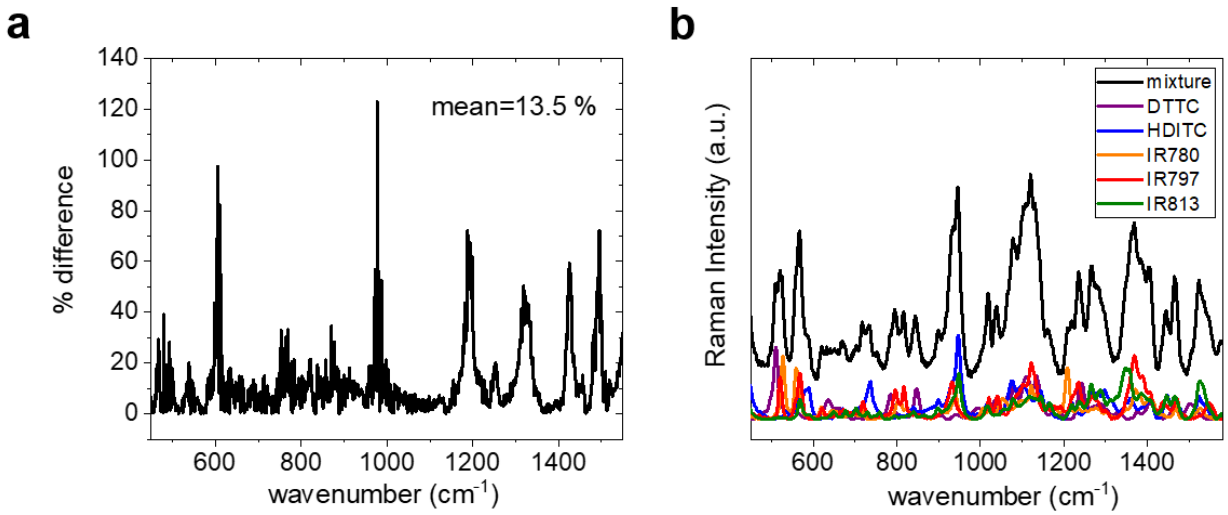

Figure S10. Spectral fitting of a five-color NIR-SERRS nanoparticle mixture. (**a**) The relative difference (% difference) between the measured and the fitted Raman spectra normalized to the measured Raman intensity (see Figure 3d in the main text). The spectral fitting error (mean=13.5%) was calculated by averaging the relative difference over the entire wavenumber range. (**b**) The fitted Raman spectrum of the NIR-SERRS nanoparticle mixture over the entire wavenumber range, which shows the linear combination of the 5 NIR-SERRS spectra (see Figure 3e in the main text). For the analysis, the 5-color NIR-SERRS nanoparticles were mixed with 1:2:3:4:5 ratio of IR813, IR780, DTTC, IR797, and HDITC-coded SERRS nanoparticles, respectively.

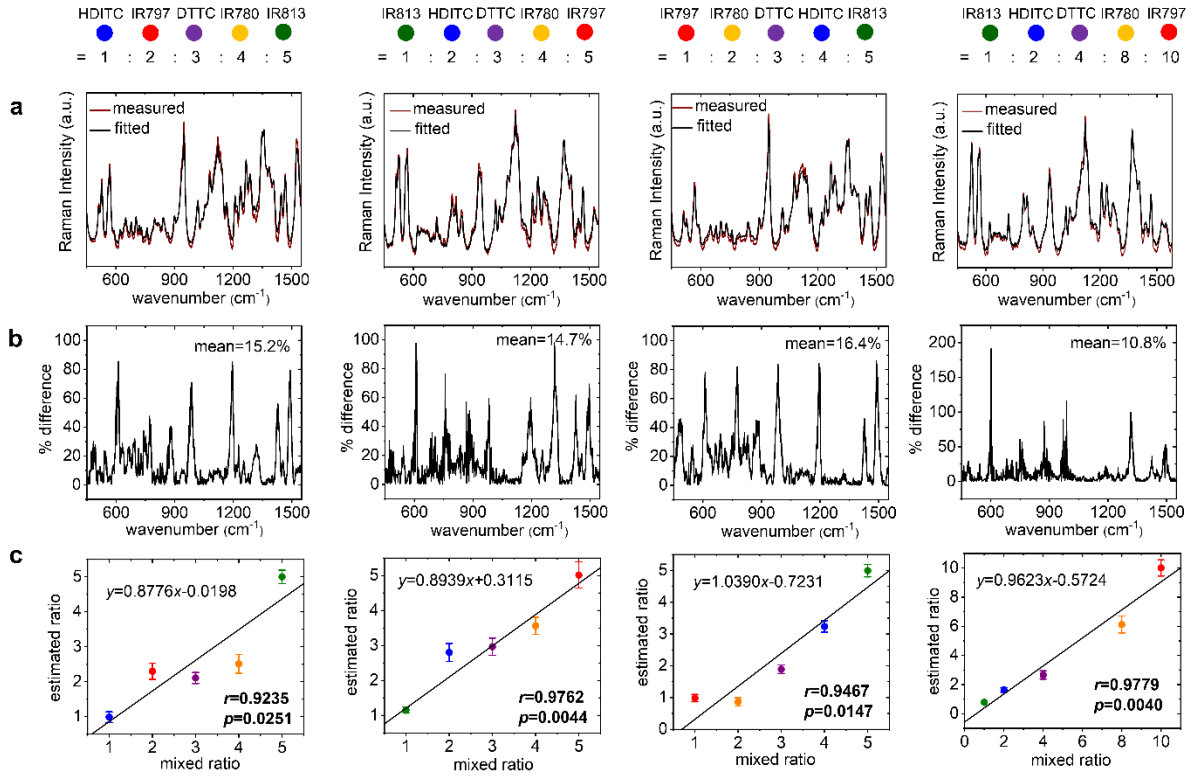

Figure S11. Spectral unmixing of various five-color NIR-SERRS nanoparticle mixtures. (**a**) Comparison between the measured Raman spectra (red) from the different ratio mixtures of the 5-color NIR-SERRS nanoparticles and their best-fitted Raman spectra (black). (**b**) The relative differences (% difference) between the measured and the fitted Raman spectra normalized to the measured Raman intensity. The spectral fitting error (mean) was calculated by averaging the relative difference over the entire wavenumber range. (**c**) The estimated ratios of the 5-color NIR-SERRS nanoparticles from the spectral unmixing of the nanoparticle mixtures, which were normalized to the average concentration of the nanoparticles of the highest amount in solutions that were set as either 5 (the left three columns) or 10 (the right column). Color codes of the 5-color NIR-SERRS nanoparticles, DTTC: purple, HDITC: blue, IR780: orange, IR797: red, and IR813: green. The error bars are the standard deviations of the nanoparticle concentrations, which were derived from the spectral unmixing of the multiple points spectra (n=300) per single mixture measurement.

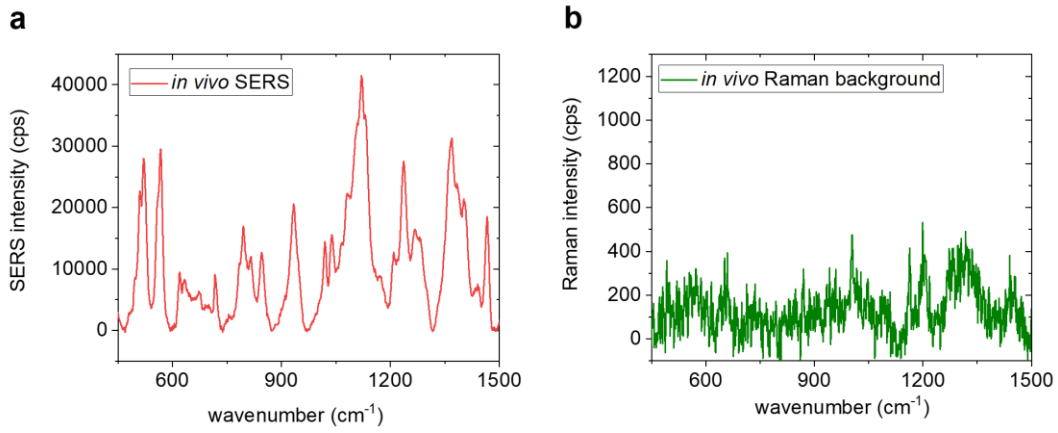

Figure S12. (**a**) *In vivo* SERS spectra of the solid tumor after the 200 μL administration of the 3 nM five-color SERRS nanoparticle mixture and (**b**) *in vivo* background Raman spectra of the living mouse obtained at the same imaging condition. Both spectra are presented after the removal of the fluorescence background.

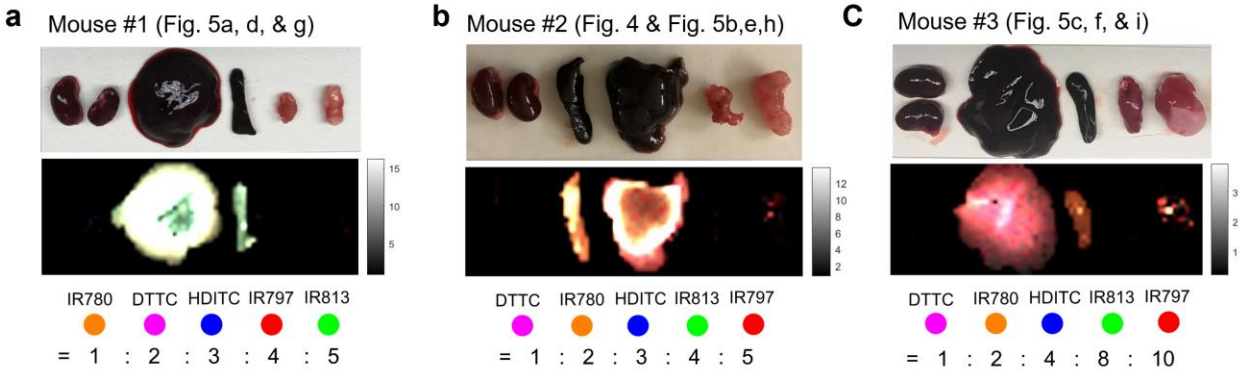

Figure S13. Bio-distribution of the five-color NIR-SERRS nanoparticles in tumor-bearing mice. (**a-c**) (from left to right) *ex vivo* five-plex Raman images of the kidneys, spleen, liver, muscle, and tumor tissue, which were obtained after 24 hours post-injection of the 5-color NIR-SERRS nanoparticles. All the images were generated through color-coding of the spectrally unmixed Raman spectra in each pixel and merging the color-coded information into one image in the same way as Figures 4 and 5 in the main text. The images were also used to calculate the biodistribution data in Fig. 4c in the main text. For the images, the mixture of 1:2:3:4:5 molar ratio of the DTTC, IR780, DTTC, HDITC, IR797, and IR813-coded SERRS nanoparticles (a), respectively, or 1:2:3:4:5 molar ratio (b) or 1:2:4:8:10 molar ratio of DTTC, IR780, HDITC, IR813, IR797-coded SERRS nanoparticles (c), respectively, was prepared and concurrently injected *via* tail-vein. Color codes of the 5-color NIR-SERRS nanoparticles, DTTC: purple, HDITC: blue, IR780: orange, IR797: red, and IR813: green. The scale bar represents Raman intensity (a.u.).

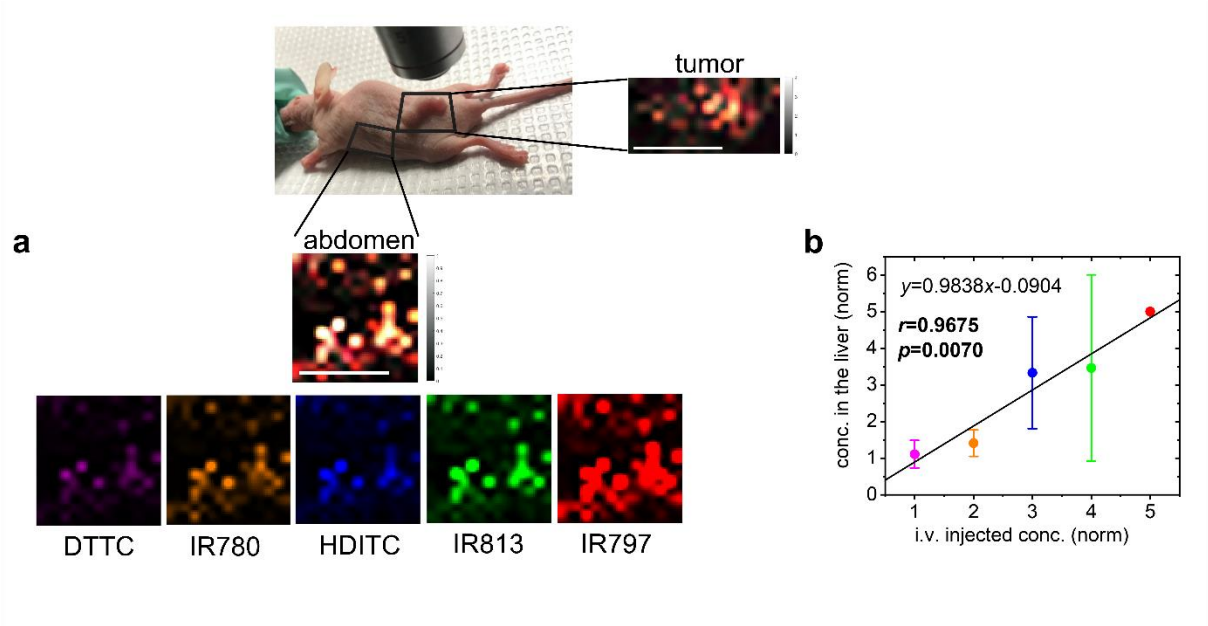

Figure S14. Noninvasive five-plex imaging of abdomen in a tumor-bearing live mouse. (**a**) *In vivo* noninvasive and multiplexed Raman image of the abdomen in a tumor-bearing mouse at 24 hrs post-injection of the 5-color NIR-SERRS nanoparticles. The same tumor xenograft nude mouse in Figure 4 (main text) was used for imaging. ROI: 15×15 mm^2, scale bar: 1 cm. The vertical scale bar on the right side of the merged image represents Raman intensity (a.u.). (**b**) The normalized concentrations (ratios) of the 5-color nanoparticles in the abdomen, obtained from the spectral unmixing of the Raman spectra in each pixel and averaged over the entire image. In each pixel, the 5-color nanoparticle concentrations were normalized to the concentration of the IR797-coded NIR-SERRS nanoparticles that was set as 5. The 5 color distribution of the NIR-SERRS nanoparticles in the abdomen matched well with the ratio of the administered nanoparticles and the 5-plex tumor image (Figure 4f and g in the main text). Color-code, DTTC: magenta-purple, IR780: orange, HDITC: blue, IR813: green., and IR797: red.

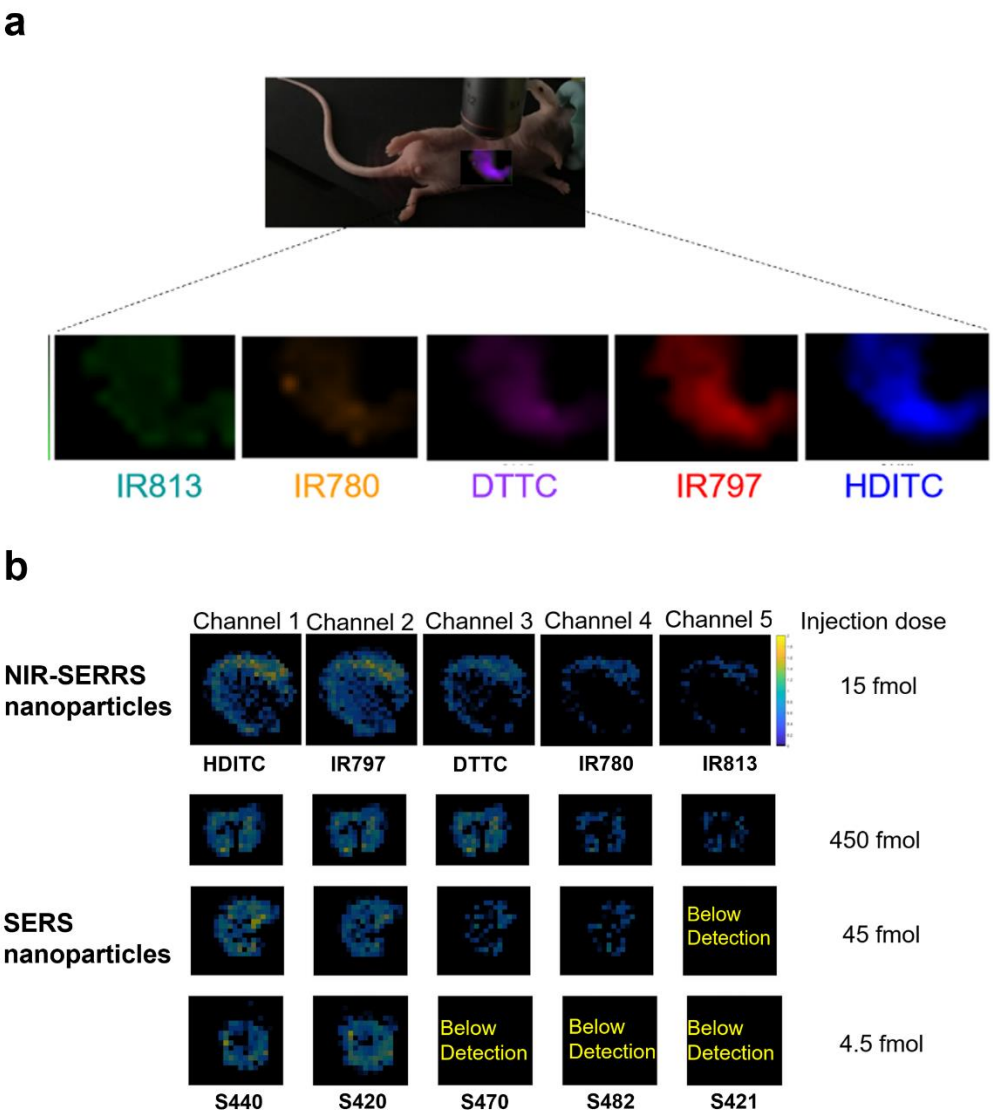

Figure S15. (**a**) *In vivo* five-plex SERS imaging of the liver after 15 fmol of the five-color NIR-SERRS nanoparticle mixture was administered. The five-color nanoparticles were mixed and intravenously injected with a 1:2:3:4:5 ratio of IR813, IR780, DTTC, IR797, and HDITC-coded nanoparticles, respectively. (**b**) Comparison of the *ex vivo* five-plex SERS images of the livers after the systematic administration of the NIR-SERRS nanoparticle mixtures (15 fmol) and the non-resonant SERS nanoparticle mixtures (450, 45, and 4.5 fmol). Channel 1 to 5 corresponds to IR813, IR780, DTTC, IR797, and HDITC-coded nanoparticles (NIR-SERRS nanoparticles) and S440, S482, S470, S420, and S421 nanoparticles (non-resonant SERS nanoparticles, see Fig. S9), which were mixed with the ratio of 5:4:3:2:1, respectively.

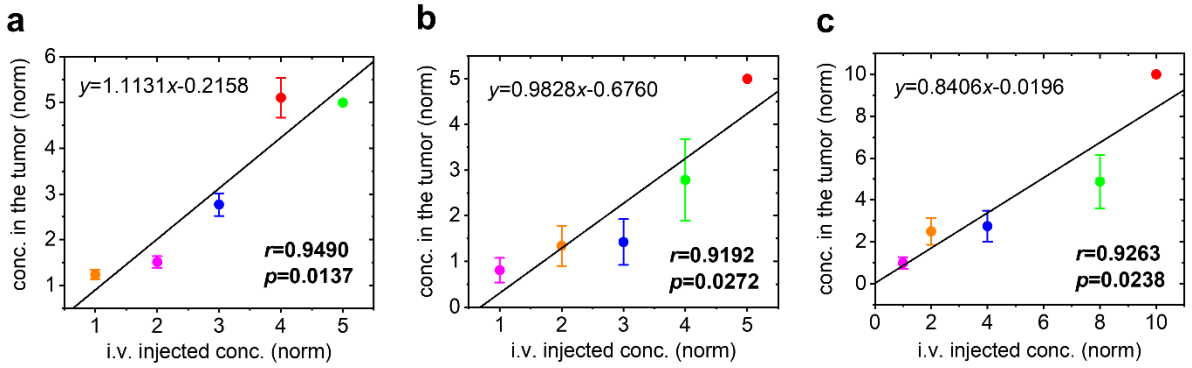

Figure S16. Spectral unmixing from the *ex vivo* five-plex images of tumors obtained after 24 hours post-injection. (**a-c**) The normalized concentrations (ratios) of the 5-color NIR-SERRS nanoparticles, which were obtained from the spectral unmixing of the Raman spectra in each pixel and averaged over the entire *ex vivo* tumor images (Figure 5g-i in the main text). The concentrations were obtained from the spectral deconvolution of the Raman spectra in each pixel and averaged over the entire images (a for mouse #1, b for mouse #2, c for mouse #3 in the main text, respectively). In each pixel, the 5-color nanoparticle concentrations were normalized to the concentration of the IR813-coded (a) or IR797-coded NIR-SERRS nanoparticles (b and c) that were set as 5 (a and b) or 10 (c). The error bars: the standard deviations of the spectrally unmixed concentrations calculated from all the pixelated Raman spectra.

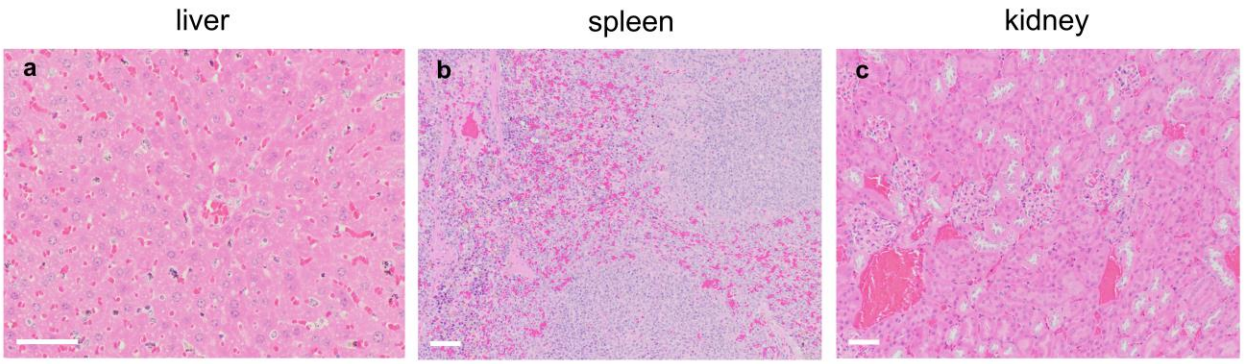

Figure S17. Histological examination of liver, spleen, and kidney with hematoxylin and eosin (×40 for liver, ×20 for spleen and kidney) obtained after multiplexed imaging of living mice, which was performed after 24 hours post-injection (n = 4). Scale bar: 50 μm. The examination confirms that there are no gross damages, inflammation, or necrosis of those organs.

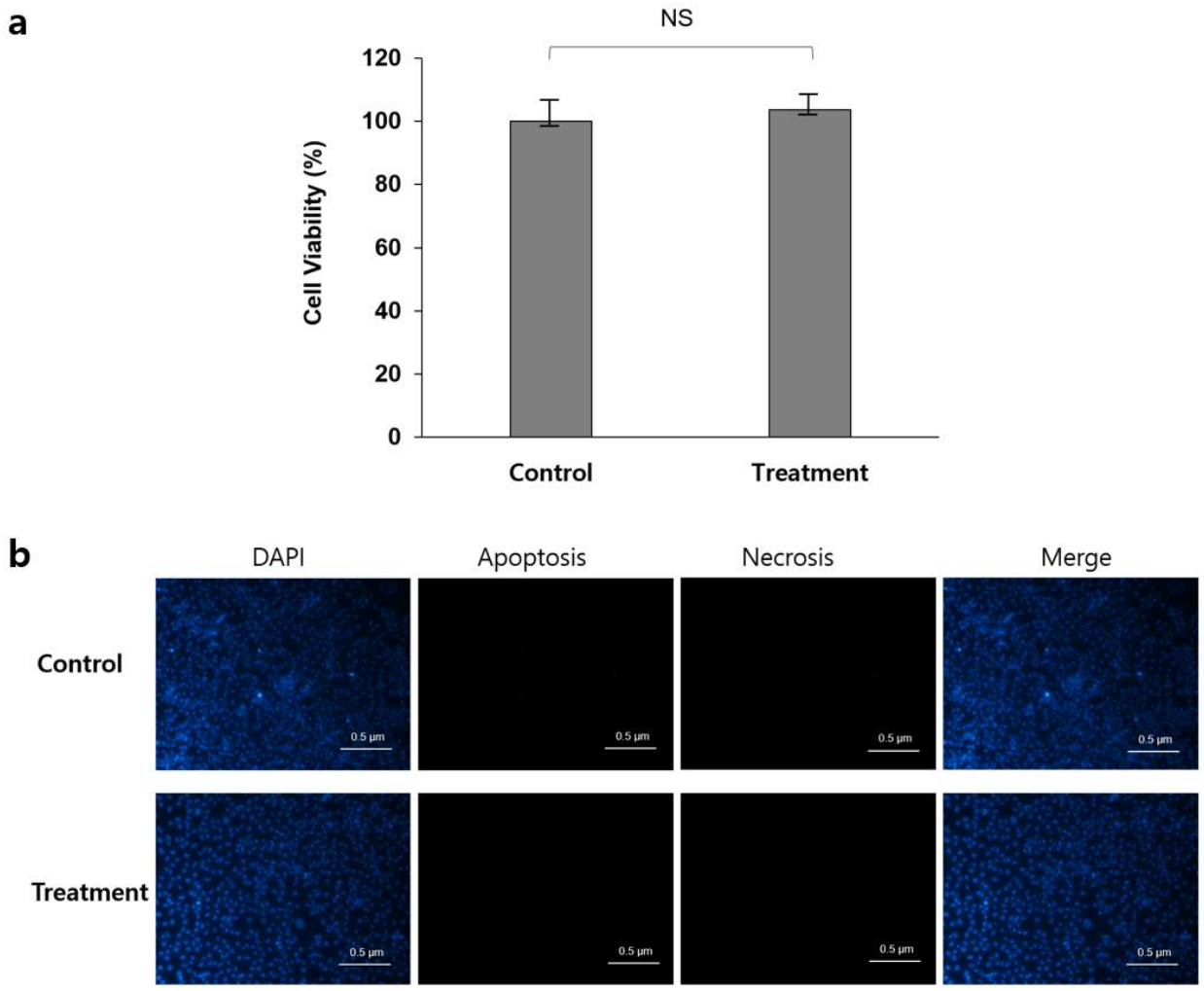

Figure S18. Cytotoxicity test of the NIR-SERRS nanoparticles. (**a**) The cell viability assay (CCK-8) for control cells and the NIR-SERRS nanoparticles-treated cells show no significant (NS) difference between the two. (**b**) The apoptosis/necrosis assay. Fluorescence images show no sign of apoptosis/necrosis for both control cells and the NIR-SERRS nanoparticles-treated cells. For the assays, 500 pM of the gold-silica NIR-SERRS oligomer nanoparticles were incubated for 48 hrs.